Mineralogical Magazine (2023), **87**, 935–942
doi:10.1180/mgm.2023.63

CAMBRIDGE UNIVERSITY PRESS

Article

Mangani-eckermannite, $NaNa_2(Mg_4Mn^{3+})Si_8O_{22}(OH)_2$, a new amphibole from Tanohata Mine, Iwate Prefecture, Japan

Anatoly V. Kasatkin[1], Natalia V. Zubkova[2], Atali A. Agakhanov[1], Nikita V. Chukanov[3], Radek Škoda[4], Fabrizio Nestola[5], Dmitry I. Belakovskiy[1] and Igor V. Pekov[2]

[1]Fersman Mineralogical Museum of the Russian Academy of Sciences, Leninsky Prospekt 18-2, 119071 Moscow, Russia; [2]Faculty of Geology, Moscow State University, Vorobievy Gory, 119991 Moscow, Russia; [3]Federal Research Center of Problems of Chemical Physics and Medicinal Chemistry of the Russian Academy of Sciences, 142432 Chernogolovka, Moscow region, Russia; [4]Department of Geological Sciences, Faculty of Science, Masaryk University, Kotlářská 2, 611 37, Brno, Czech Republic; and [5]Dipartimento di Geoscienze, Università di Padova, Via Gradenigo 6, I-35131, Padova, Italy

Abstract

Mangani-eckermannite, ideally $NaNa_2(Mg_4Mn^{3+})Si_8O_{22}(OH)_2$, is a new member of the amphibole supergroup found at Tanohata Mine, Shimohei District, Iwate Prefecture, Japan. It occurs as prismatic crystals up to 0.3 × 0.2 mm and their aggregates up to 1 mm intergrown with braunite, vittinkiite and quartz. Mangani-eckermannite is cherry-red to very dark red and reddish-brown in thicker grains. It is translucent with a pinkish white streak and vitreous lustre. It is brittle, fracture is stepped along crystal elongation and uneven across a crystal. Cleavage is perfect on {110}. Mohs hardness is 6. D_{meas} = 3.16(2) and D_{calc} = 3.186 g/cm^3. The mineral is optically biaxial (–), with α = 1.645(3), β = 1.668(2), γ = 1.675(3) (589 nm); $2V_{meas}$ = 60(10)°, $2V_{calc}$ = 57°. The empirical formula derived from electron microprobe analysis, secondary-ion mass spectrometry and single-crystal structure refinement and calculated on the basis of 24 (O+OH) atoms per formula unit (apfu) is $^{A}(Na_{0.74}K_{0.24}\square_{0.02})_{\Sigma1.00}{}^{B}(Na_{1.52}Ca_{0.24}Mn^{2+}_{0.24})_{\Sigma2.00}{}^{C}(Mg_{2.54}Mn^{2+}_{1.45}Mn^{3+}_{0.71}Fe^{3+}_{0.26}Ti_{0.04})_{\Sigma5.00}{}^{T}(Si_{7.97}Al_{0.03})_{\Sigma8.00}O_{22}{}^{W}[(OH)_{1.52}O_{0.48}]_{\Sigma2.00}$. Mangani-eckermannite is monoclinic, space group *C*2/*m*, *a* = 9.9533(4), *b* = 18.1440(7), *c* = 5.2970(2) Å, β = 103.948(4)°, *V* = 928.39(6) Å^3 and *Z* = 2. The strongest lines of the powder X-ray diffraction pattern [*d*, Å (*I*, %)(*hkl*)] are: 8.52(100)(110); 4.54(25)(040); 3.41(29)(131); 3.16(23)(310,201); 2.721(37)(151); 2.533(26)(2̄02). The crystal structure was refined to R_1 = 0.0264 for 1001 independent reflections with $I > 2\sigma(I)$. The place of mangani-eckermannite in the nomenclature of the amphibole supergroup is discussed and the status of mangano-ferri-eckermannite as a valid mineral species and successor of 'kôzulite' is questioned.

Keywords: mangani-eckermannite; new mineral; amphibole supergroup; crystal structure; silicate manganese ore; Tanohata Mine

(Received 9 May 2023; accepted 6 August 2023; Accepted Manuscript published online: 10 August 2023; Associate Editor: Mihoko Hoshino)

Introduction

The amphibole supergroup includes numerous minerals with the general chemical formula $AB_2C_5T_8O_{22}W_2$, where A = vacancy, Na, K, Ca, Pb and Li; B = Na, Ca, Mn^{2+}, Fe^{2+}, Mg and Li; C = Mg, Fe^{2+}, Mn^{2+}, Al, Fe^{3+}, Mn^{3+}, Ti^{4+} and Li; T = Si, Al, Ti^{4+} and Be; and W = (OH), F, Cl and O^{2-} (Hawthorne *et al.*, 2012). The new member of the supergroup characterised as a new mineral species in this paper has been named mangani-eckermannite (Russian Cyrillic: манганиэкерманнит), in accordance with the current amphibole nomenclature scheme. The root-name 'eckermannite' is applied to the following end-member composition $^{A}Na^{B}Na_2{}^{C}(Mg_4Al)^{T}Si_8O_{22}{}^{W}(OH)_2$ (Hawthorne *et al.*, 2012; Oberti *et al.*, 2015b) while the prefix 'mangani-' is added because Mn^{3+} is dominant amongst trivalent cations in C positions.

The new mineral, its name and symbol (Meck) have been approved by the Commission on New Minerals, Nomenclature and Classification of the International Mineralogical Association (IMA2023-004; Kasatkin *et al.*, 2023). The holotype specimen is deposited in the collections of the Fersman Mineralogical Museum of the Russian Academy of Sciences, Moscow, Russia with the registration number 5774/1.

Corresponding author: Anatoly V. Kasatkin; Email: anatoly.kasatkin@gmail.com
Cite this article: Kasatkin A.V., Zubkova N.V., Agakhanov A.A., Chukanov N.V., Škoda R., Nestola F., Belakovskiy D.I. and Pekov I.V. (2023) Mangani-eckermannite, $NaNa_2(Mg_4Mn^{3+})Si_8O_{22}(OH)_2$, a new amphibole from Tanohata Mine, Iwate Prefecture, Japan. *Mineralogical Magazine* **87**, 935–942. https://doi.org/10.1180/mgm.2023.63

Occurrence and mineral association

The new mineral occurs at No. 3 orebody (also known as Matsumaezawa Pit) of the Tanohata Mine, Shimohei District, Iwate Prefecture, Japan (39°55"N, 141°54"E). This manganese orebody is located in the upper-Jurassic accretionary complex chert and underwent contact metamorphism by the intrusion of granodiorite (Nambu *et al.*, 1969a). The orebody has a metasomatic origin and zoned structure. The dominant zones are composed mainly of braunite, rhodonite, quartz, natronambulite and serandite, while a thin amphibole-rich zone is wedged between them (Nishio-Hamane *et al.*, 2014). A more detailed geological description of the Tanohata Mine was reported by Nambu *et al.* (1969b). Tanohata Mine is the type locality for mangano-ferri-eckermannite (first described as 'kôzulite' by Nambu *et al.*, 1969a: see Discussion section), natronambulite (Matsubara *et al.*, 1985), potassic-ferri-leakeite

(first described as 'potassicleakeite' by Matsubara *et al.*, 2002), watatsumiite (Matsubara *et al.*, 2003), tanohataite (Nagase *et al.*, 2012) and iwateite (Nishio-Hamane *et al.*, 2014).

The specimen containing mangani-eckermannite was obtained by the senior author in the early 2000s as 'kôzulite' and was stored in his systematic mineral collection until the recent investigation showed it to be a new mineral.

Mangani-eckermannite is associated closely with braunite, vittinkiite, albite and quartz.

General appearance and physical properties

Mangani-eckermannite occurs as prismatic crystals up to 0.3×0.2 mm and their aggregates up to 1 mm intergrown with braunite, vittinkiite and quartz (Figs 1 and 2). The colour of the new mineral is cherry-red to very dark red; in thicker grains it is reddish-brown. Mangani-eckermannite is translucent with a pinkish white streak and vitreous lustre. It is brittle, fracture is stepped along crystal elongation and uneven across a crystal. Cleavage is perfect on {110}. No fluorescence is observed under long- or short-wave ultraviolet light. Mohs hardness is 6 based on scratch tests. Density measured by flotation in Clerici solution is 3.16(2) g/cm^3; the density value calculated using the empirical formula and unit-cell volume obtained from single-crystal X-ray diffraction (XRD) data is 3.186 g/cm^3.

The new mineral is brown in transmitted light. Thicker grains are reddish brown. It is optically biaxial (–), with $\alpha = 1.645(3)$, $\beta = 1.668(2)$ and $\gamma = 1.675(3)$ (589 nm). The estimated 2V angle based on the conoscopical isogyre curve in the sections perpendicular to optical axes is 60(10)°, the calculated 2V value is 57°. Dispersion of optical axes is not observed but could be masked by the saturated colour of the mineral. Mangani-eckermannite is weakly pleochroic in brown colours, with $Z \approx Y > X$. Twinning was observed with the twinning plane parallel to crystal elongation. The elongation is positive. The crystals which show twinning have a parallel extinction.

Spectroscopical studies

Infrared spectroscopy

In order to obtain the infrared (IR) absorption spectrum, a powdered mangani-eckermannite sample was mixed with anhydrous KBr, pelletised, and analysed using an ALPHA FTIR spectrometer (Bruker Optics) in the range of 360–3800 cm^{-1}, at a resolution of 4 cm^{-1}. A total of 64 scans were collected. The IR spectrum of an analogous pellet of pure KBr was used as a reference. The assignment of absorption bands in the IR spectrum of mangani-eckermannite (Fig. 3) is as follows: weak bands in the range of 3600–3800 cm^{-1} correspond to O–H stretching vibrations; and bands of Si–O stretching vibrations are observed in the range of 900–1140 cm^{-1}. The ranges of 580–790 and 370–460 cm^{-1} correspond to overlapping bands of O–Si–O and M···O–H bending modes and overlapping bands of M···O stretching and Si–O–Si bending modes, respectively where M = Mg, Mn or Fe and '···' denotes a noncovalent (ionic) bond.

The assignment of the bands of O–H stretching vibrations was carried out taking into account occupancies of sites coordinating OH groups ($Mg_{0.655}Mn_{0.345}$ for *M*1 and $Mg_{0.812}Mn_{0.188}$ for *M*3: see below) and data taken from literature sources.

For potassium-fluor-richterite and K-rich richterites, the band of stretching vibrations of OH groups belonging to the cluster MgMgMg–OH–(K) is observed in the range from 3694 to 3730 cm^{-1} (Della Ventura *et al.*, 1992, 1998; Gottschalk and Andrut, 1998). In the IR spectrum of synthetic end-member potassium richterite this band is observed at 3734 cm^{-1} (Hawthorne, 1995).

As a result of annealing of Mn–bearing arfvedsonite in air, the OH stretching band of the (MgMgMg)–OH–A–OH configuration shifts downward from 3730 to near 3700 cm^{-1} with formation of the (MgMgMg)–OH–A–O configuration due to dehydrogenation of OH at the O3 site (Ishida and Hawthorne, 2001). According to Ishida and Hawthorne (2001), wavenumbers of O–H stretching bands of richteritic amphiboles (M = Fe or Mn) are 3644–3640 cm^{-1} for the (Mg$R^{2+}R^{2+}$)–OH–□ configuration and 3643 cm^{-1} for the (MgMgR^{3+})–OH–□ configuration. According to Oberti *et al.* (2006), the assignments of OH-stretching bands for parvo-mangano-edenite is as follows:

3692 cm^{-1} for AlSi–(MgMgMn)–OH–^{A}Na,
3693 cm^{-1} for SiSi–(MgMgMn)–OH–^{A}Na,
3672 cm^{-1} for SiSi–(MgMgMg)–OH–^{A}□,
3677 cm^{-1} for SiSi–(MnMnMn)–OH–^{A}Na,

Figure 1. A 0.7 cm thick vein consisting of dark red mangani-eckermannite intergrown with black braunite, pink vittinkiite and colourless albite in a rock mainly consisting of colourless to pale salmon-reddish quartz. Holotype sample #5774/1, size: 2 × 1.5 × 1.5 cm. Photo: M. Milshina.

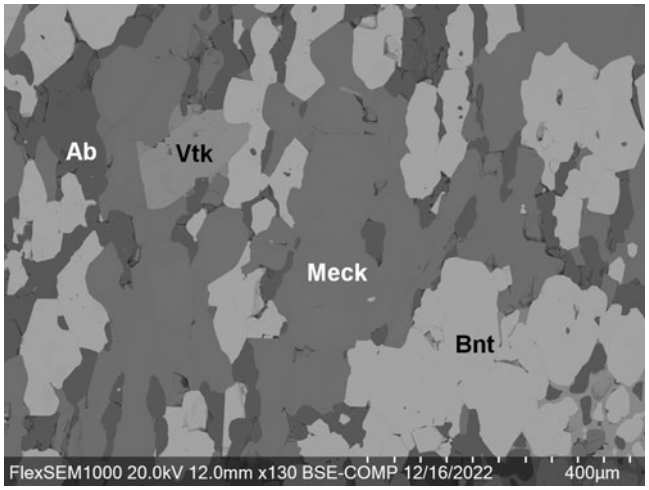

Figure 2. Anhedral grains of mangani-eckermannite (Meck) closely intergrown with braunite (Bnt), albite (Ab) and vittinkiite (Vtk). Polished section. Back-scattered electron image.

https://doi.org/10.1180/mgm.2023.63 Published online by Cambridge University Press

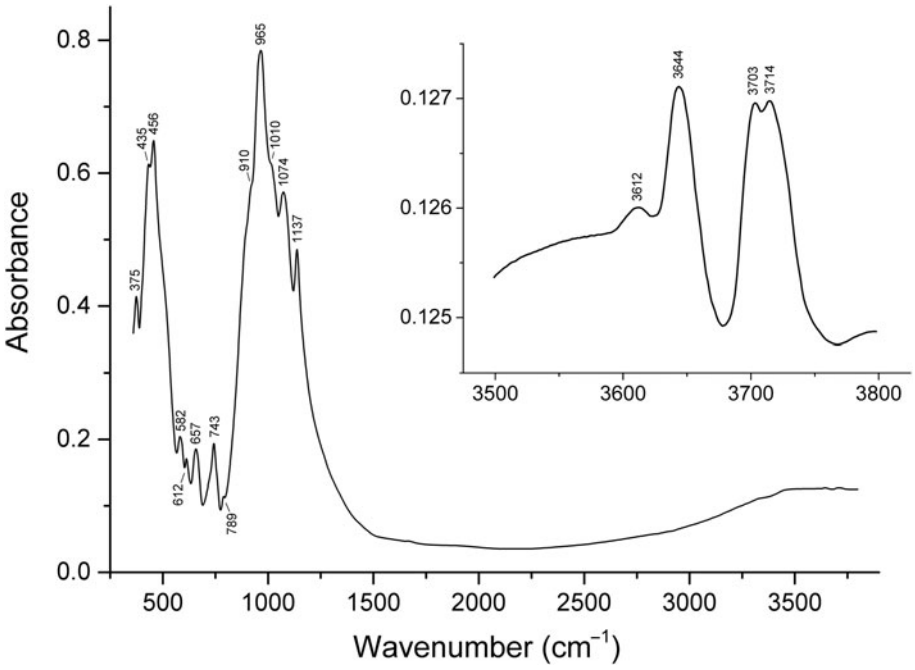

Figure 3. Powder infrared absorption spectrum of mangani-eckermannite.

3659 cm^{-1} for SiSi–(MgMgMn)–OH–^{A}□
3641 cm^{-1} for SiSi–(MgMnMn)–OH–^{A}□

A similar band assignment was made by Hawthorne and Della Ventura (2007). Generally, substitution of M^{2+} for M^{3+} in the local environment of the OH group results in the 30–40 cm^{-1} shift of the OH-stretching band towards lower frequencies.

On the basis of these data and trends and taking into account relative band intensities, OH-stretching bands in the IR spectrum of mangani-eckermannite have been assigned to the following configurations:

3714 cm^{-1} – (MgMgMg)–OH–^{A}Na
3703 cm^{-1} – (MgMgMn^{2+})–OH–^{A}Na
3644 cm^{-1} – (MgMn^{2+}Mn^{2+})–OH–^{A}Na and/or (MgMgMn^{3+})–OH–^{A}Na
3612 cm^{-1} – (MgMn^{2+}Mn^{3+})–OH–^{A}Na and/or (MgMn^{2+}Fe^{3+})–OH–^{A}Na

Raman spectroscopy

The Raman spectrum of mangani-eckermannite (Fig. 4) was obtained by means of a Horiba Labram HR Evolution spectrometer. This dispersive, edge-filter-based system is equipped with an Olympus BX 41 optical microscope, a diffraction grating

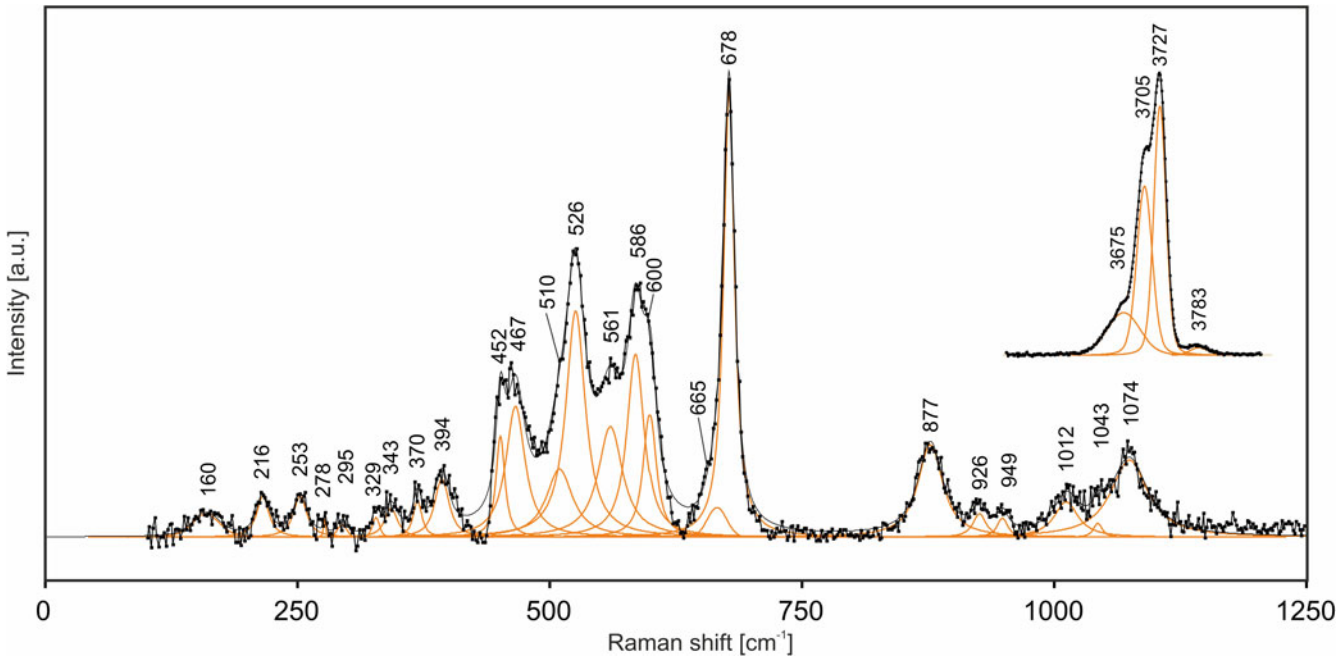

Figure 4. Raman spectrum of mangani-eckermannite excited by a 532 nm laser: in the 100–1250 cm^{-1} region and in the 2500–4000 cm^{-1} region (inset in the upper right corner). The measured spectrum is shown by dots. The curve matched to the dots is a result of spectral fit as a sum of individual Voigt peaks shown below the curve.

https://doi.org/10.1180/mgm.2023.63 Published online by Cambridge University Press

Table 1. Chemical composition of mangani-eckermannite.

Constituent	Wt.%	Range	S.D.	Reference material
Na_2O	7.93	7.80–8.06	0.09	Amelia albite
K_2O	1.26	1.08–1.34	0.09	sanidine
MgO	11.60	11.40–12.00	0.22	pyrope
CaO	1.55	1.47–1.65	0.06	wollastonite
MnO*	13.55	18.75–19.43**	0.25**	rhodonite
Mn_2O_3*	6.33			
Fe_2O_3	2.31	1.88–2.52	0.21	almandine
Al_2O_3	0.20	0.16–0.24	0.03	almandine
SiO_2	54.18	53.63–54.57	0.31	almandine
TiO_2	0.32	0.28–0.35	0.03	titanite
H_2O***	1.55	1.53–1.57	0.015	
Total	100.78			

*Apportioned from 19.24 wt.% MnO measured by electron microprobe analysis
**For total Mn calculated as MnO.
***Calculated from 0.172 wt.% H (mean of 5 spots; range 0.170–0.174; S.D. 0.002) determined by SIMS.
S.D. = Standard deviation

Table 2. Powder X-ray diffraction data (d in Å) of mangani-eckermannite.

I	$d_{meas.}$(Å)	d_{calc}(Å)	h	k	l
100	**8.52**	8.527	1	1	0
9	4.89	4.886	$\bar{1}$	1	1
25	**4.54**	4.536	0	4	0
4	4.27	4.263	2	2	0
6	4.02	4.039	$\bar{2}$	0	1
		4.039	1	1	1
7	3.88	3.887	$\bar{1}$	3	1
2	3.68	3.690	$\bar{2}$	2	1
29	**3.41**	3.418	1	3	1
12	3.30	3.306	2	4	0
23	**3.16**	3.170	3	1	0
		3.160	2	0	1
10	2.980	2.984	2	2	1
3	2.942	2.952	$\bar{1}$	5	1
7	2.830	2.842	3	3	0
37	**2.721**	2.730	1	5	1
13	2.599	2.606	0	6	1
4	2.568	2.570	0	0	2
26	**2.533**	2.537	$\bar{2}$	0	2
2	2.499	2.503	1	7	0
3	2.401	2.408	3	5	0
11	2.344	2.350	$\bar{3}$	5	1
		2.340	$\bar{4}$	2	1
6	2.304	2.308	$\bar{1}$	7	1
		2.290	3	3	1
8	2.275	2.279	$\bar{3}$	1	2
3	2.212	2.214	$\bar{2}$	4	2
12	2.180	2.185	2	6	1
6	2.142	2.147	$\bar{3}$	3	2
8	2.068	2.071	2	0	2
3	2.040	2.044	3	5	1
5	2.016	2.020	$\bar{4}$	0	2
		2.019	2	2	2
		2.019	3	7	0
3	1.967	1.971	1	5	2
		1.960	4	2	1
2	1.916	1.921	5	1	0
2	1.886	1.890	$\bar{4}$	6	1
		1.887	4	6	0
3	1.868	1.874	$\bar{1}$	9	1
2	1.834	1.836	4	4	1
2	1.808	1.813	1	9	1
4	1.750	1.753	$\bar{5}$	1	2
3	1.738	1.740	1	7	2
8	1.689	1.691	$\bar{2}$	8	2
9	1.668	1.673	4	6	1
6	1.649	1.653	4	8	0
4	1.623	1.626	1	11	0

with 600 grooves per millimetre, and a Peltier-cooled, Si-based charge-coupled device (CCD) detector. The Raman signal was excited by 532 nm laser with the beam power of 10 mW at the sample surface. Raman signal was collected in the range of 100–4000 cm^{-1} with a 50× objective and the system being operated in the confocal mode, beam diameter was ~2.6 μm and the axial resolution ~5 μm. Time acquisition was 60 s per spectral frame and 4 accumulations were applied. Wavenumber calibration was done using the Rayleigh line and low-pressure Ne-lamp emissions. The wavenumber accuracy was ~0.5 cm^{-1}, and the spectral resolution was ~2 cm^{-1}. Band fitting was done after appropriate background correction, assuming combined Lorentzian–Gaussian band shapes using the Voight function (*PeakFit*; Jandel Scientific Software).

The assignment of Raman bands of mangani-eckermannite is analogous to the assignment of its IR absorption bands:

Bands at 3727 and 3705 and 3675 cm^{-1} correspond to O–H stretching vibrations in the prevailing (MgMgMg)–OH–^{A}Na and (MgMgMn^{2+})–OH–^{A}Na local environments, respectively. The broad band at 3675 cm^{-1} observed as a shoulder in the overall spectrum, may be due to the superposition of bands corresponding to the (MgMn^{2+}Mn^{2+})–OH–^{A}Na and (MgMgMn^{3+})–OH–^{A}Na configurations.

A very weak peak at 3783 cm^{-1} cannot be associated to an O–H stretching fundamental mode, but theoretically it may correspond to a combination (lattice + O–H stretching) mode. Intensities of bands corresponding to other local environments are below the detection limits.

Bands of Si–O stretching vibrations are observed in the range of 800–1100 cm^{-1}.

The ranges of 500–700 and 370–470 cm^{-1} correspond to overlapping bands of O–Si–O and M···O–H bending modes and overlapping bands of M···O stretching and Si–O–Si bending modes, respectively.

Bands below 370 cm^{-1} are due to lattice modes involving Na···O stretching vibrations and bending vibrations of Na- and M-centred polyhedra.

Chemical composition

Seven electron-microprobe analyses were carried out with a Cameca SX-100 electron microprobe (WDS mode with an accelerating voltage of 15 kV, a beam current on the specimen of 10 nA and a beam diameter of 4 μm). Peak counting times (CT) were 20 s for all elements; CT for each background was one-half of the peak time. The raw intensities were converted into concentrations using *X-PHI* (Merlet, 1994) matrix-correction software. The H_2O content was calculated from hydrogen content measured using secondary-ion mass spectrometry (SIMS) at Cameca IMS 4F. Lithium, beryllium and boron were sought after but their contents measured by SIMS were found to be below the detection limits of this method. The presence of OH^- groups and the absence of B–O, C–O and N–O bonds in the mineral is also confirmed by IR and Raman spectroscopic data.

Analytical data and standards used are given in Table 1.

The empirical formula, calculated on the basis of 24 anions (O+OH) per formula unit, is $Na_{2.26}K_{0.24}Ca_{0.24}Mg_{2.54}Mn^{2+}_{1.69}Mn^{3+}_{0.71}Fe^{3+}_{0.26}Ti_{0.04}Al_{0.03}Si_{7.97}O_{22.48}(OH)_{1.52}$. All Fe was considered as Fe^{3+} due to the presence of Mn^{3+} and redox potential

https://doi.org/10.1180/mgm.2023.63 Published online by Cambridge University Press

Table 3. Single-crystal X-ray diffraction data collection information and structure refinement parameters for mangani-eckermannite.

Empirical formula	$^{A}(Na_{0.74}K_{0.24})_{\Sigma 0.98}{}^{B}(Na_{1.52}Ca_{0.24}Mn^{2+}_{0.24})_{\Sigma 2.00}{}^{C}(Mg_{2.54}Mn^{2+}_{1.45}Mn^{3+}_{0.71}Fe^{3+}_{0.26}Ti_{0.04})_{\Sigma 5.00}$ $^{T}(Si_{7.97}Al_{0.03})_{\Sigma 8.00}O_{22}{}^{W}[(OH)_{1.52}O_{0.48}]_{\Sigma 2.00}$
Formula weight	891.22
Temperature (K)	293(2)
Radiation and wavelength (Å)	Mo$K\alpha$; 0.71073
Crystal system, space group (Z)	Monoclinic, $C2/m$, 2
Unit cell dimensions (Å/°)	a = 9.9533(4)
	b = 18.1440(7)
	c = 5.2970(2)
	β = 103.948(4)
V (Å^3)	928.39(6)
Absorption coefficient μ (mm^{-1})	2.743
F_{000}	876
Crystal size (mm)	0.037 × 0.105 × 0.215
Diffractometer	Rigaku SuperNova with Pilatus 200K
θ range for data collection (°) / Collection mode	2.39–28.28 / full sphere
Index ranges	$-13 \le h \le 13$, $-24 \le k \le 24$, $-7 \le l \le 7$
Reflections collected	10835
Independent reflections	1182 (R_{int} = 0.0535; R_{sigma} = 0.0284)
Independent reflections with $I>2\sigma(I)$	1001
Data reduction	*CrysAlisPro* 1.171.41.123a (Rigaku Oxford Diffraction, 2022)
Absorption correction	Multi-scan
Refinement method	Full-matrix least-squares on F^2
Number of refined parameters	111
Final R indices [$I>2\sigma(I)$]	R_1 = 0.0264, wR_2* = 0.0654
R indices (all data)	R_1 = 0.0335, wR_2* = 0.0684
GoF	1.030
Largest diff. peak and hole (e/Å^3)	0.44 (at 0.72 Å from O2) and −0.37 (at 0.99 Å from $M2$)

*$w = 1/[\sigma^2(F_o^2) + (0.0371P)^2 + 0.4615P]$; $P = ([\text{max of } (0 \text{ or } F_o^2)] + 2F_c^2)/3$

arguments, whereas the Mn^{2+}:Mn^{3+} ratio was calculated from charge-balance requirements. At the next step, we filled the T and C sites in order to yield 13 cations: Si and Al were placed in T sites while Mg, Fe, Ti, Mn^{3+} and partly Mn^{2+} where placed in C, in accordance with the common scheme for amphiboles. After these positions were filled, some Mn^{2+} still remained and was placed in the B position – in very good agreement with the structure data that indicated more electrons than Na+Ca could give there. All the above results in the following chemical formula re-written according to the requirements of the current amphibole nomenclature (Hawthorne *et al.*, 2012): $^{A}(Na_{0.74}K_{0.24}\square_{0.02})_{\Sigma 1.00}$ $^{B}(Na_{1.52}Ca_{0.24}Mn^{2+}_{0.24})_{\Sigma 2.00}{}^{C}(Mg_{2.54}Mn^{2+}_{1.45}Mn^{3+}_{0.71}Fe^{3+}_{0.26}Ti_{0.04})_{\Sigma 5.00}$ $^{T}(Si_{7.97}Al_{0.03})_{\Sigma 8.00}O_{22}{}^{W}[(OH)_{1.52}O_{0.48}]_{\Sigma 2.00}$.

The ideal formula is $NaNa_2(Mg_4Mn^{3+})Si_8O_{22}(OH)_2$,which requires Na_2O 11.18, MgO 19.38, Mn_2O_3 9.48, SiO_2 57.79, H_2O 2.17, total 100 wt.%.

The Gladstone–Dale compatibility index calculated based on the empirical formula and unit-cell parameters from the single-crystal XRD data is $1 - (K_p/K_c) = 0.007$ using D_{meas} and 0.015 using D_{calc}. Both values are rated as superior and indirectly but convincingly confirm the correctness of our chemical data, including the calculation of the Mn^{2+}/Mn^{3+} ratio, the presence of iron in trivalent state and the determination of H_2O content. For details on the application of the compatibility concept in mineralogy see (Mandarino, 1981) and references therein.

Table 4. Atom coordinates, equivalent isotropic displacement parameters (in Å^2) and site occupancy factors (s.o.f.) for mangani-eckermannite.

Site	x	y	z	U_{eq}	s.o.f.
$M1$	0.0	0.08665(3)	½	0.0144(2)	$Mg_{0.655(5)}Mn_{0.345(5)}$
$M2$	0.0	0.18224(2)	0.0	0.01416(17)	$Mn_{0.802(5)}Mg_{0.198(5)}$
$M3$	0.0	0.0	0.0	0.0128(4)	$Mg_{0.812(6)}Mn_{0.188(6)}$
$T1$	0.27978(5)	0.08423(3)	0.28892(10)	0.01263(16)	$Si_{1.00}$
$T2$	0.28684(5)	0.16930(3)	0.79295(10)	0.01316(15)	$Si_{1.00}$
$M4$	0.0	0.27224(5)	½	0.0251(4)	$Na_{0.806(5)}Mn_{0.194(5)}$
Am	0.0227(13)	½	0.0607(16)	0.068(4)	$Na_{0.527(15)}$
$A2$	0.0	0.464(3)	0.0	0.030(14)*	$Na_{0.047(14)}$
O1	0.11421(14)	0.08483(7)	0.2152(3)	0.0146(3)	$O_{1.00}$
O2	0.12030(14)	0.16779(8)	0.7198(3)	0.0178(3)	$O_{1.00}$
O3	0.10509(19)	0.0	0.7122(4)	0.0159(4)	$O_{1.00}$
H	0.1987(11)	0.0	0.753(8)	0.019*	$H_{0.76}$**
O4	0.36037(15)	0.24630(8)	0.7896(3)	0.0226(3)	$O_{1.00}$
O5	0.34537(13)	0.12764(7)	0.0782(2)	0.0176(3)	$O_{1.00}$
O6	0.34279(13)	0.11618(8)	0.5802(2)	0.0184(3)	$O_{1.00}$
O7	0.3390(2)	0.0	0.2873(4)	0.0203(4)	$O_{1.00}$

* U_{iso}

** The position of H atom was found from difference Fourier synthesis and O3–H distance was restrained softly to be 0.90(1) and U_{iso}H = 1.2U_{eq}O3. The site occupancy factor for the H atom was fixed according to the chemical formula.

X-ray diffraction data and crystal structure

The powder XRD data (Table 2) were obtained using RKU-86 mm camera with Cr$K\alpha$ radiation, V-filter and using Ge as an internal standard. The unit-cell parameters refined from the powder data using *UNITCELL* software by Holland and Redfern (1997) are as follows: mangani-eckermannite is monoclinic, space group $C2/m$, a = 9.920(5), b = 18.112(4), c = 5.2920(4) Å, β = 103.97(4)°, V = 923(1)Å^3 and Z = 2.

To collect the single-crystal XRD data a crystal of mangani-eckermannite, 0.04 × 0.11 × 0.22 mm in size, extracted from the polished section analysed using electron microprobe and SIMS, was mounted on a glass fibre and examined with a Supernova Rigaku-Oxford Diffraction diffractometer equipped with a micro-source Mo$K\alpha$ radiation (λ = 0.71073 Å; 50 kV and 0.8 mA) and a Pilatus 200K Dectris detector. The sample-to-detector distance was set to 68 mm. The data were collected by 1855 frames over 43 runs; the exposure time was 30 s per frame. The data were processed by *CrysAlisPro 1.171.41.123a* software (Rigaku Oxford

https://doi.org/10.1180/mgm.2023.63 Published online by Cambridge University Press

Table 5. Selected interatomic distances (in Å) in the crystal structure of mangani-eckermannite.

*M*1–O3	2.0645(13) ×2	*M*3–O3	2.0462(18) ×2	*T*1–O1	1.5994(14)	*Am*–O7	2.417(11)
*M*1–O2	2.0699(14) ×2	*M*3–O1	2.0823(13) ×4	*T*1–O5	1.6258(13)	*Am*–O7	2.553(10)
*M*1–O1	2.0966(13) ×2	<*M*3–O>	2.070	*T*1–O6	1.6258(14)	*Am*–O5	2.845(6) ×2
<*M*1–O1>	2.077			*T*1–O7	1.6388(8)	*Am*–O5	2.927(8) ×2
		*M*4–O4	2.3294(14) ×2	<*T*1–O>	1.622	*Am*–O6	2.937(7) ×2
*M*2–O4	2.0267(14) ×2	*M*4–O2	2.3891(16) ×2			<*Am*–O>	2.80
*M*2–O2	2.1360(13) ×2	*M*4–O6	2.6549(16) ×2	*T*2–O4	1.5792(15)		
*M*2–O1	2.2563(13) ×2	<*M*4–O>	2.458	*T*2–O2	1.6091(14)	*A*2–O5	2.37(4) ×2
<*M*2–O1>	2.140			*T*2–O5	1.6643(13)	*A*2–O7	2.546(15) ×2
				*T*2–O6	1.6768(14)	*A*2–O6	2.80(3) ×2
				<*T*2–O>	1.632	<*A*2–O>	2.57

Table 6. Bond-valence analysis (values given in valence units) for mangani-eckermannite. Bond valence parameters from Gagné and Hawthorne (2015).*

Site	*M*1	*M*2	*M*3	*T*1	*T*2	*M*4	*Am*	*A*2	Σ
O1	$0.35^{\times 2\downarrow}$	$0.26^{\times 2\downarrow}$	$0.35^{\times 4\downarrow}$	1.07					2.03
O2	$0.38^{\times 2\downarrow}$	$0.35^{\times 2\downarrow}$			1.04	$0.22^{\times 2\downarrow}$			1.99
O3 = OH,O	$0.39^{\times 2\downarrow \times 2\rightarrow}$		$0.37^{\times 2\downarrow}$						1.15
O4		$0.47^{\times 2\downarrow}$			1.12	$0.24^{\times 2\downarrow}$			1.83
O5				1.00	0.90		$0.04^{\times 2\downarrow}$, $0.03^{\times 2\downarrow}$	$0.01^{\times 2\downarrow}$	1.98
O6				1.00	0.87	$0.11^{\times 2\downarrow}$	$0.03^{\times 2\downarrow}$		2.01
O7				$0.96^{\times 2\rightarrow}$			0.11, 0.07	$0.01^{\times 2\downarrow \times 2\rightarrow}$	2.12
Σ	2.24	2.16	2.14	4.03	3.93	1.14	0.38	0.04	

*Note: Bond-valence calculations were performed taking into account the assigned site occupancies of Table 7.

Diffraction). The mineral is monoclinic, $C2/m$, $a = 9.9533(4)$, $b = 18.1440(7)$, $c = 5.2970(2)$ Å, $\beta = 103.948(4)°$, $V = 928.39(6)$ Å^3 and $Z = 2$.

The crystal structure of mangani-eckermannite was solved from single-crystal X-ray data and refined with the use of the *SHELX* software package (Sheldrick, 2015) to $R_1 = 0.0264$ for 1001 independent reflections with $I > 2\sigma(I)$. Crystal data, data collection information and structure refinement details are given in Table 3, coordinates and equivalent isotropic displacement parameters of atoms in Table 4, selected interatomic distances in Table 5. Bond-valence sums are given in Table 6. Assigned site occupancies based on the results of the crystal structure refinement are given in Table 7. The crystallographic information file has been deposited with the Principal Editors of *Mineralogical Magazine* and is available as Supplementary material (see below).

The crystal structure of mangani-eckermannite, similar to other amphiboles, is based on double chains of corner-sharing tetrahedra $[T_4O_{11}]^{\infty}$ running along the *c* axis. Adjacent double chains are linked *via* the strips built by *M*1–3-centred octahedra. *M*4-centred octahedra are located at the periphery of *M*1–3 octahedral strips. The *A* cations occupy the centre of the large cavity and are moved from the centre of the cavity with point symmetry 2/*m* to the *A*2 and *Am* sites, which is typical for amphiboles (Hawthorne *et al.*, 2012).

The refinement of occupancies for the *M*1–3 sites was performed for Mg *vs.* Mn and results in the following values of the refined number of electrons (e_{ref}): 16.49, 22.43 and 14.44 for *M*1, *M*2 and *M*3, respectively. Refinement of the *M*4 site was performed for Na *vs.* Mn and gave $e_{ref} = 13.72$. Site occupancy factors of the *Am* and *A*2 sites were refined using the Na scattering curve and gave e_{ref} values of 5.80 and 0.52, respectively. Final site occupancies are given in Table 7. They are based on the results of the crystal structure refinement, analysis of interatomic distances, bond valence calculations and chemical composition.

Relationship to other species and the status of mangano-ferri-eckermannite

Mangani-eckermannite is another new member of the amphibole supergroup (Hawthorne *et al.*, 2012). At lower hierarchical levels, it belongs to the sodium amphiboles subgroup within the group of ^{W}(OH,F,Cl)-dominant amphiboles. It is the Mn^{3+}-dominant analogue of eckermannite $^{A}Na^{B}Na_2^{C}(Mg_4Al)^{T}Si_8O_{22}{}^{W}(OH)_2$ (Oberti *et al.*, 2015b) and magnesio-arfvedsonite $^{A}Na^{B}Na_2{}^{C}(Mg_4Fe^{3+})$ $^{T}Si_8O_{22}{}^{W}(OH)_2$ (Oberti *et al.*, 2015a). For the comparison of the three species see Table 8.

Though manganese is a rather common component in amphiboles, in most cases it is present just as a small admixture. 'Mangani-amphiboles' i.e. those having Mn^{3+} as a dominant component amongst trivalent cations in C positions, are rare. Mangani-eckermannite is the seventh member of the amphibole supergroup with Mn^{3+} as a species-defining cation, after potassic-mangani-leakeite $KNa_2(Mg_2Mn_2^{3+}Li)Si_8O_{22}(OH)_2$ (Armbruster *et al.*, 1993 as "kornite"; renamed by Hawthorne *et al.*, 2012), mangano-mangani-ungarettiite $NaNa_2(Mn_2^{2+}Mn_3^{3+})Si_8O_{22}O_2$

Table 7. Site occupancies proposed for mangani-eckermannite based on the results of the crystal structure refinement.

Site	Refined site occupancies	SSF_{exp} (e^-)	Assigned site occupancies	SSF_{calc} (e^-)
*M*1	$Mg_{0.655(5)}Mn_{0.345(5)}$	16.49	$Mg_{0.66}Mn_{0.06}^{2+}Mn_{0.13}^{3+}$ $Fe_{0.13}^{3+}Ti_{0.02}$	16.49
*M*2	$Mn_{0.802(5)}Mg_{0.198(5)}$	22.43	$Mg_{0.20}Mn_{0.63}^{2+}Mn_{0.17}^{3+}$	22.40
*M*3	$Mg_{0.812(6)}Mn_{0.188(6)}$	14.44	$Mg_{0.82}Mn_{0.07}^{2+}Mn_{0.11}^{3+}$	14.34
*M*4	$Na_{0.806(5)}Mn_{0.194(5)}$	13.72	$Na_{0.76}Mn_{0.12}^{2+}Ca_{0.12}$	13.76
Am	$Na_{0.527(15)}$	5.80	$Na_{0.32}K_{0.12}$	5.80
*A*2	$Na_{0.047(14)}$	0.52	$Na_{0.05}$	0.55

SSF_{exp} and SSF_{calc} are the experimental and calculated site-scattering factors normalised to unity, respectively.

https://doi.org/10.1180/mgm.2023.63 Published online by Cambridge University Press

Table 8. Comparative data for mangani-eckermannite, eckermannite and magnesio-arfvedsonite.

Mineral	Mangani-eckermannite	Eckermannite	Magnesio-arfvedsonite
Ideal formula	$NaNa_2(Mg_4Mn^{3+})Si_8O_{22}(OH)_2$	$NaNa_2(Mg_4Al)Si_8O_{22}(OH)_2$	$NaNa_2(Mg_4Fe^{3+})Si_8O_{22}(OH)_2$
Crystal system	Monoclinic	Monoclinic	Monoclinic
Space group	*C*2/*m*	*C*2/*m*	*C*2/*m*
a (Å)	9.9533(4)	9.8087(7)	9.867(1)
b (Å)	18.1440(7)	17.8448(13)	17.928(2)
c (Å)	5.2970(2)	5.2905(4)	5.284(1)
β (°)	103.948(4)	103.660(1)	103.80(2)
V (Å^3)	928.39(6)	899.8(1)	907.7(2)
Z	2	2	2
Strongest lines of the powder	8.52–100	8.407–42	8.451–46
X-ray diffraction pattern:	4.54–25	3.395–59	3.399–68
d, Å – *I*, %	3.41–29	3.128–56	3.273–39
	3.16–23	2.702–100	3.144–63
	2.721–37	2.574–36	2.708–100
	2.533–26	2.525–56	2.526–60
Density (g cm^{-3}):			
Measured	3.16(2)	No data	No data*
Calculated	3.186	3.02	3.034
Hardness	6	6	No data*
Optical data:			
Optical sign	Biaxial (–)	Biaxial (–)	Biaxial (–)
α	1.645(3)	1.605(2)	1.624(2)
β	1.668(2)	1.630(2)	1.636(2)
γ	1.675(3)	1.634(2)	1.637(2)
2V (measured) (°)	60(10)	43.0(5)	36(1)
2V (calculated) (°)	57.1	43	32
Pleochroism	Weak, in brown tint. $Z \approx Y > X$	*X* = medium grey, *Y* = pale grey to colourless, *Z* = light grey; $X > Z > Y$	*X* = light grey, *Y* = dark grey, *Z*= medium grey; $Y > Z > X$
Source	This paper	Oberti *et al.* (2015b)	Oberti *et al.* (2015a)

*For the type specimen described by Oberti *et al.* (2015a)

(Hawthorne *et al.*, 1995 as "ungarettiite"; renamed by Hawthorne *et al.*, 2012), mangani-obertiite $NaNa_2(Mg_3Mn^{3+}Ti^{4+})Si_8O_{22}O_2$ (Hawthorne *et al.*, 2000 as "obertiite"; renamed by Williams *et al.*, 2014), mangani-dellaventuraite $NaNa_2(MgMn_2^{3+}Ti^{4+}Li)Si_8O_{22}O_2$ (Tait *et al.*, 2005 as "dellaventuraite"; renamed by Hawthorne *et al.*, 2012), oxo-mangani-leakeite $NaNa_2(Mn_4^{3+}Li)Si_8O_{22}O_2$ (Oberti *et al.*, 2016) and mangani-pargasite $NaCa_2(Mg_4Mn^{3+})(Si_6Al_2)O_{22}(OH)_2$ (Hålenius *et al.*, 2020). All these amphiboles occur mainly in metamorphosed manganese deposits.

As mentioned above, the specimen of the new mineral described in this paper was initially received with the label 'kôzulite'. The latter was described from Tanohata Mine by Nambu *et al.* (1969a) without structure description. Kitamura and Morimoto (1972) presented the structure refinement of a kôzulite crystal with the composition $(Na_{2.54}K_{0.27}Ca_{0.19})(Mn_{3.69}Mg_{0.63}Fe^{3+}_{0.33}Al_{0.31})Si_{8.00}O_{21.789}[(OH)_{2.18}F_{0.04}]$, however, they did not report detailed structure information, such as atomic coordinates and displacement parameters, as well as the valence of Mn. Later, Barkley *et al.* (2010) refined the structure of kôzulite giving the ideal formula as $NaNa_2[Mn_4^{2+}(Fe^{3+},Al)]Si_8O_{22}(OH)_2$. After the adoption of the current amphiboles nomenclature (Hawthorne *et al.*, 2012), kôzulite was redefined to mangano-ferri-eckermannite (see, *e.g.*, Oberti *et al.*, 2015b). The official IMA-CNMNC List of Mineral Names (Pasero, 2023, http://cnmnc.main.jp/) includes mangano-ferri-eckermannite as a valid mineral species referring to Barkley *et al.* (2010) and Hawthorne *et al.* (2012). However, the empirical chemical formula was reported by Barkley *et al.* (2010) as $(K_{0.20}Na_{0.80})_{\Sigma1.00}(Na_{1.60}Ca_{0.18}Mn^{2+}_{0.22})_{\Sigma2.00}(Mn^{2+}_{2.14}Mn^{3+}_{0.25}Mg_{2.20}Fe^{3+}_{0.27}Al_{0.14})_{\Sigma5.00}(Si_{7.92}Al_{0.06}Ti_{0.02})_{\Sigma8.00}O_{22}[(OH)_{1.86}F_{0.14}]_{\Sigma2.00}$, i.e. it has Mg > Mn^{2+} and Fe^{3+} > Mn^{3+} > Al as C-cations and, thus, formally corresponds to magnesio-arfvedsonite but not mangano-ferri-eckermannite. This questions the existence of mangano-ferri-eckermannite as a valid mineral species (although, it can exist as a so-called 'named amphibole'), at least, as applied to the sample studied by Barkley *et al.* (2010). It is obvious from the data that this sample was not a part of the original material studied by Nambu *et al.* (1969a) and Kitamura and Morimoto (1972) whose 'kôzulite' is obviously a 'mangano-eckermannitic' amphibole with only 0.63 Mg vs. 3.69 Mn apfu. However, the absence of structural data and the Mn^{2+}:Mn^{3+} ratio does not allow assigning of their mineral to a particular mineral species.

It should be also noted that the data reported by Barkley *et al.* (2010) show very close Mg and Mn^{2+} values (2.20 *vs.* 2.14 apfu) as well as Fe^{3+} and Mn^{3+} values (0.27 *vs.* 0.25 apfu). This means that their sample might contain local compositions corresponding to different amphibole species including the mangani-eckermannite described here. More recently, Nishio-Hamane *et al.* (2022) studied another sample of 'kôzulite' from Tanohata Mine and found it to be mangano-mangani-ungarettiite and 'mangano-mangani-eckermannite', a potentially new mineral. Thus 'kôzulites' should be subjected to chemical and structural studies to be correctly assigned to a particular mineral species. Nishio-Hamane *et al.* (2022) also stated that all samples of 'kôzulite' investigated earlier had dark red and reddish black colours, whereas mangano-ferri-eckermannite might exist but should be sought after in orange-coloured specimens.

Acknowledgements. We acknowledge Associate Editor Mihoko Hoshino, Sergey Aksenov and two anonymous reviewers and Principal Editor Stuart Mills for valuable comments. The IR spectroscopy investigation and

https://doi.org/10.1180/mgm.2023.63 Published online by Cambridge University Press

interpretation of the Raman spectrum were carried out in accordance with the state task of the Russian Federation, state registration No. AAAA-A19-119092390076-7.

Supplementary material. The supplementary material for this article can be found at https://doi.org/10.1180/mgm.2023.63.

Competing interests. The authors declare none.

References

Armbruster T., Oberhänsli R., Bermanec V. and Dixon R. (1993) Hennomartinite and kornite, two new Mn^{3+} rich silicates from the Wessels mine, Kalahari, South Africa. *Schweizerische Mineralogische und Petrographische Mitteilungen*, **73**, 349–355.

Barkley M.C., Yang H. and Downs R.T. (2010) Kôzulite, an Mn-rich alkali amphibole. *Acta Crystallographica*, **E66**, i83.

Della Ventura G., Parodi G.C., Maras A. and Mottana A. (1992) Potassium-fluor-richterite, a new amphibole from San Vito, Monte Somma, Campania, Italy. *Rendicondi Lincei, Scienze Fisiche*, **3**, 239–245.

Della Ventura G., Robert J.-L. and Hawthorne F.C. (1998) Characterization of OH-F short-range order in potassium-fluor-richterite by infrared spectroscopy in the OH-stretching region. *The Canadian Mineralogist*, **36**, 181–185.

Gagné O.C. and Hawthorne F.C (2015) Comprehensive derivation of bond-valence parameters for ion pairs involving oxygen. *Acta Crystallographica*, **B71**, 562–578.

Gottschalk M. and Andrut M. (1998) Structural and chemical characterization of synthetic (Na, K)-richterite solid solutions by EMP, HRTEM, XRD and OH-valence vibrational spectroscopy. *Physics and Chemistry of Minerals*, **25**, 101–111.

Hålenius U., Bosi F. and Jonsson E. (2020) Mangani-pargasite, $NaCa_2(Mg_4Mn^{3+})(Si_6Al_2)O_{22}(OH)_2$, a new mineral species of the amphibole supergroup. *Periodico di Mineralogia*, **89**, 125–131.

Hawthorne F.C. (1995) Entropy-driven disorder in end-member amphiboles. *The Canadian Mineralogist*, **33**, 1189–1204.

Hawthorne F.C. and Della Ventura G. (2007) Short-range order in amphiboles. Pp. 173–222 in: *Amphiboles: Crystal-Chemistry, Occurrence and Health Issues* (Hawthorne F.C., Oberti R., Della Ventura G. and Mottana, A., editors). Reviews in Mineralogy and Geochemistry, **67**. Mineralogical Society of America and the Geochemical Society, Chantilly, Virginia, USA.

Hawthorne F.C., Oberti R., Cannillo E., Sardone N., Zanetti A., Grice J.D. and Ashley P.M. (1995) A new anhydrous amphibole from the Hoskins mine, Grenfell, New South Wales, Australia: Description and crystal structure of ungarettiite, $NaNa_2(Mn^{2+}_2Mn^{3+}_3)Si_8O_{22}O_2$. *American Mineralogist*, **80**, 165–172.

Hawthorne F.C., Cooper M.A., Grice J.D. and Ottolini L. (2000) A new anhydrous amphibole from the Eifel region, Germany: Description and crystal structure of obertiite, $NaNa_2(Mg_3Fe^{3+}Ti^{4+})Si_8O_{22}O_2$. *American Mineralogist*, **85**, 236–241.

Hawthorne F.C., Oberti R., Harlow G.E., Maresch W.V., Martin R.F., Schumacher J.C. and Welch M.D. (2012) Nomenclature of the amphibole supergroup. *American Mineralogist*, **97**, 2031–2048.

Holland T.J.B. and Redfern S.A.T. (1997) Unit cell refinement from powder diffraction data: the use of regression diagnostics. *Mineralogical Magazine*, **61**, 65–77.

Ishida K. and Hawthorne F.C. (2001) Assignment of infrared OH-stretching bands in manganoan magnesio-arfvedsonite and richterite through heat-treatment. *American Mineralogist*, **86**, 965–972.

Kasatkin A.V., Zubkova N.V., Agakhanov A.A., Chukanov N.V., Škoda R., Nestola F., Belakovskiy D.I. and Pekov I.V. (2023) Mangani-eckermannite, IMA 2023-004. CNMNC Newsletter 73. *Mineralogical Magazine*, **87**, https://doi.org/10.1180/mgm.2023.44

Kitamura M. and Morimoto N. (1972) Crystal structure of kôzulite and tetrahedral Al in amphiboles. *Acta Crystallographica*, **A28**, S71.

Mandarino J.A. (1981) The Gladstone–Dale relationship. IV. The compatibility concept and its application. *The Canadian Mineralogist*, **19**, 441–450.

Matsubara S., Kato A. and Tiba T. (1985) Natronambulite, (Na,Li)(Mn, $Ca)_4Si_5O_{14}OH$, a new mineral from the Tanohata mine, Iwate Prefecture, Japan. *Mineralogical Journal*, **12**, 332–340.

Matsubara S., Miyawaki R., Kurosawa M. and Suzuki Y. (2002) Potassicleakeite, a New Amphibole from the Tanohata Mine, Iwate Prefecture, Japan. *Journal of Mineralogical and Petrological Sciences*, **97**, 177–184.

Matsubara S., Miyawaki R., Kurosawa M. and Suzuki Y. (2003) Watatsumiite, $KNa_2LiMn_2V_2Si_8O_{24}$, a new mineral from the Tanohata mine, Iwate Prefecture, Japan. *Journal of Mineralogical and Petrological Sciences*, **98**, 142–150.

Merlet C. (1994) An accurate computer correction program for quantitative electron probe microanalysis. *Microchimica Acta*, **114/115**, 363–376.

Nagase T., Hori H., Kitamine M., Nagashima M., Abduriyim A. and Kuribayashi T. (2012) Tanohataite, $LiMn_2Si_3O_8(OH)$: a new mineral from the Tanohata mine, Iwate Prefecture, Japan. *Journal of Mineralogical and Petrological Sciences*, **107**, 149–154.

Nambu M., Tanida K. and Kitamura T. (1969a) Kôzulite, a new alkali amphibole, from Tanohata mine, Iwate prefecture, Japan. *Journal of the Japanese Association of Mineralogists, Petrologists and Economic Geologists*, **62**, 311–328 [in Japanese with English abstract].

Nambu M., Tanida K. and Kumagai S. (1969b) *Manganese Deposits in Kitakami Mountainland. I, Iwate Prefecture*, pp.146 [in Japanese].

Nishio-Hamane D., Minakawa T. and Okada H. (2014) Iwateite, $BaNa_2Mn(PO_4)_2$, a new mineral from Tanohata mine, Iwate Prefecture, Japan. *Journal of Mineralogical and Petrological Sciences*, **109**, 34–37.

Nishio-Hamane D., Momma K., Ohnishi M., Norimasa S., Minakawa T., Okada H. and Imai H. (2022) Mangano-mangani-ungarettiite from Tanohata mine, Iwate Prefecture, Japan. 2022 *Annual Meeting of Japan Association of Mineralogical Sciences*, R1P-11 [in Japanese], https://confit.atlas.jp/guide/event/jams2022/subject/R1P-11/detail

Oberti R., Cámara F., Della Ventura G., Iezzi G. and Benimoff A.I. (2006) Parvo-mangano-edenite, parvo-manganotremolite, and the solid-solution between Ca and Mn^{2+} at the *M*4 site in amphiboles. *American Mineralogist*, **91**, 526–532.

Oberti R., Boiocchi M., Hawthorne F.C., Ball N.A. and Harlow G.E. (2015a) Magnesio-arfvedsonite from Jade Mine Tract, Myanmar: mineral description and crystal chemistry. *Mineralogical Magazine*, **79**, 253–260.

Oberti R., Boiocchi M., Hawthorne F.C., Ball N.A. and Harlow G.E. (2015b) Eckermannite revised: The new holotype from the Jade Mine Tract, Myanmar—crystal structure, mineral data, and hints on the reasons for the rarity of eckermannite. *American Mineralogist*, **100**, 909–914.

Oberti R., Boiocchi M., Hawthorne F.C., Ball N.A. and Ashley P.M. (2016) Oxo-mangani-leakeite from the Hoskins mine, New South Wales, Australia: occurrence and mineral description. *Mineralogical Magazine*, **80**, 1013–1021.

Pasero M. (2023) *The New IMA List of Minerals.* International Mineralogical Association Commission on new minerals, nomenclature and classification (IMA-CNMNC). http://cnmnc.main.jp/.

Rigaku Oxford Diffraction (2022) *CrysAlisPro Software System, Version 1.171.41.123a.*

Sheldrick G.M. (2015) Crystal structure refinement with SHELXL. *Acta Crystallographica*, **C71**, 3–8.

Tait K.T., Hawthorne F.C., Grice J.D., Ottolini L. and Nayak V.K. (2005) Dellaventuraite, $NaNa_2(MgMn^{3+}_2Ti^{4+}Li)Si_8O_{22}O_2$, a new anhydrous amphibole from the Kajlidongri Manganese Mine, Jhabua District, Madhya Pradesh, India. *American Mineralogist*, **90**, 304–309.

Williams P.A., Hatert F., Pasero M. and Mills S.J. (2014) IMA Commission on New Minerals, Nomenclature and Classification (CNMNC) Newsletter 22. New minerals and nomenclature modifications approved in 2014. *Mineralogical Magazine*, **78**, 1241–1248.